METEOROLOGICAL APPLICATIONS
Meteorol. Appl. **20**: 466–481 (2013)
Published online 30 March 2012 in Wiley Online Library
(wileyonlinelibrary.com) DOI: 10.1002/met.1311

RMetS
Royal Meteorological Society

A climatology of lee waves over the UK derived from model forecasts

S. B. Vosper,* H. Wells, J. A. Sinclair and P. F. Sheridan
Met Office, Exeter, UK

ABSTRACT: A lee wave forecast system has been run operationally at the UK Met Office since 2006. The forecasts are produced by a numerical model for flow over complex terrain (3DVOM) which is run for five separate hilly regions across the UK. These regions cover Dartmoor (southwest England), Snowdonia (north Wales), Cumbria and the Pennines (northern England), the Grampians (Scotland) and the Mourne and Sperrin mountains (Northern Ireland). Examples of verification of the model forecasts against aircraft and satellite observations are presented. Three years of forecast data for these regions have been used to generate a lee wave climatology for the UK. The model predicts large geographical differences, with lee waves occurring least frequently over Dartmoor and most frequently over Snowdonia and the Grampians. Large amplitude waves, with peak vertical velocities exceeding 3 m s^{-1} at 700 hPa or above, are more common in forecasts for the Grampian region than others. Lee waves occur more frequently in forecasts during winter months than in summer. The most favourable conditions are those in which there is little turning of the lower tropospheric winds and analysis suggests that the waves are typically trapped in the lower troposphere. The influence of the lee waves on the near-surface flow has also been investigated. Large accelerations and flow deflections can occur beneath the waves. It is suggested that the latter correspond to turbulent lee wave rotors. Preferred locations for this behaviour have been identified in the model forecasts for the Grampians and Pennines.

KEY WORDS gusts; mountain wave; orography; rotor

Received 25 November 2011; Revised 25 January 2012; Accepted 27 February 2012

1. Introduction

Internal gravity waves generated by flow over orography, otherwise known as mountain waves, or lee waves, are of interest for a number of reasons. From a safety perspective, it is well known that lee waves can pose a hazard to aviation. The up- and downdraughts associated with large-amplitude waves are problematic for light aircraft, particularly at low levels over mountainous terrain, and the severe turbulence which occurs in regions of wave breaking has been cited as the cause of damage to aircraft (e.g. NTSB, 1993), and occasional fatal accidents (e.g. NTSB, 1992). Near the ground the waves may give rise to strong acceleration of the flow, resulting in rapid spatial and temporal changes in wind speed and direction. This can be problematic at airfields (e.g. Mobbs *et al*., 2005; Sheridan *et al*., 2007) and for road transport, where the strong gusts associated with the waves are known to overturn high-sided vehicles. Extreme conditions are associated with rotors, horizontally orientated vortices which form beneath the crests of waves. Rotors contain severe turbulence and wind shear and are considered to be highly dangerous for aviation. They have been the focus of considerable recent study. Research programmes such as The Terrain-induced Rotor Experiment (T-REX) are leading to new insight into the conditions under which rotors form and the mechanisms which control their behaviour (Grubišić *et al*., 2008).

Lee waves are also used widely by glider pilots to achieve high altitudes and distances. Away from the regions of wave breaking and low-level rotors the flow in a lee wave field is generally laminar. The wave motion may remain steady for several hours and the updraughts are therefore ideal for maintaining (or increasing) altitude and flying very long distances. World record flight performances have been made in the waves generated by several mountain ranges around the world (e.g. the European Alps, the Sierra Nevada, USA and the Argentinean Andes).

The importance of lee waves suggests that climatological information about their occurrence and geographical distribution could be of considerable value. Evidence for wave motion can often be observed in high-resolution visible satellite imagery over the UK, manifested as quasi-linear bands of cloud oriented approximately perpendicular to the flow (e.g. Galvin and Owens, 2006; Galvin *et al*., 2006; Galvin, 2009). Such satellite images can be used to establish a climatology of wave activity, and indeed this has been done successfully in the past (Lester, 1978; Grubišić and Billings, 2008). However, these techniques are limited by the extent to which cloud patterns can be used to determine the presence of wave motion. Waves will remain undetected in clear sky cases and the generally coarser resolution of infra-red satellite imagery means that little or no information is available at night. Radiosondes have been used extensively to observe and measure the properties of lee waves (e.g. Shutts *et al*., 1994; Vosper and Mobbs, 1996). The fluctuations in balloon ascent rate can provide accurate estimates of the vertical velocities associated with the wave motion. However, the infrequent and localized sampling of such observations means that they are not well suited to establishing climatological information. In the absence of a technique which can sample both the spatial and temporal variations of wave activity, the predictions of a numerical model might be considered a suitable substitute.

This paper describes the development of a lee wave climatology from the predictions of a numerical model. The lee wave

* Correspondence to: S. B. Vosper, Met Office, FitzRoy Road, Exeter, Devon EX1 3PB, UK. E-mail: simon.vosper@metoffice.gov.uk

model, 3DVOM (Three-Dimensional Velocities Over Mountains), has been used operationally at the UK Met Office for forecasting lee waves since May 2006.

The layout of the paper is as follows. Section 2 describes the model and provides some example verification of the predictions against observations. The operational forecast system is described in Section 3 and comparisons with satellite imagery are presented in Section 4. Section 5 describes the climatological analysis of the forecast lee waves and their impact on the near-surface flow is investigated in Section 6. A summary is presented in Section 7.

2. The 3DVOM lee wave forecast model

3DVOM is a finite-difference numerical model designed for high-resolution simulations of lee waves generated by flow over complex terrain. The basic form of the model is documented by Vosper (2003). A brief overview, along with a description of more recent developments, is given here.

In order to produce forecasts for multiple areas in a timely fashion, without the need for significant computing resources, it is necessary to use a simplified set of equations. The model is based on the linearized shallow Boussinesq equations of motion for a dry atmosphere, linearized about a background profile of wind and potential temperature (assumed to be dependent on height only). The linear approximation is generally valid for small amplitude waves and is a reasonable one provided the mountain slopes are small and the non-dimensional mountain height NH/U, where N is the buoyancy frequency, U is the wind speed and H is the mountain height, is less than unity (Smith, 1980, 1988). In practice, this condition is satisfied much of the time for UK mountain ranges during the windy conditions for which lee waves are expected to occur. This will be demonstrated in Section 3 by examining the NH/U distribution across different regions. It should be noted, however, that even under conditions of $NH/U \ll 1$ nonlinearity can still have a significant effect if the waves are strongly trapped, causing unsteadiness in the wave field (Nance and Durran, 1998) and for mountains which are wide (relative to the lee wave horizontal wavelength), determining the amplitude (e.g. Durran, 1992; Vosper, 2004). The neglect of moisture effects in the model may also have some implications for accuracy. Previous studies (e.g. Durran and Klemp, 1982) have demonstrated how, for two-dimensional lee waves in idealized two-layer flows, the presence of moisture can significantly alter the lee waves, either amplifying, re-tuning or destroying the trapped wave response. Such effects cannot be represented by 3DVOM. However, the nonlinear nature of the moisture effect makes it difficult to estimate how this is likely to impact on either the model performance, or the climatology of lee waves. It is noteworthy that, in spite of the lack of moist processes in the model, good agreement is obtained between the model and observations for the moist case study presented below.

The UK Met Office now uses a variable-resolution configuration of its Unified Model with a 1.5 km horizontal grid spacing over the UK for operational forecasting. In principle, a large portion of the gravity wave spectrum can be resolved on such a grid. However, other aspects of numerical weather prediction (NWP) models can make them unsuitable for representing gravity waves. For example, the temporal off-centring commonly used in semi-implicit numerical schemes can, when combined with the relatively long model timesteps required for efficient operational use, have an adverse damping effect on gravity wave motion (Shutts and Vosper, 2011). There is therefore still a need for simplified models.

An extension of the model presented by Vosper (2003) is the transformation of the equations onto a terrain-following vertical co-ordinate. The transformed linear equations are discretized using second-order accurate centred differencing and integrated forward in time using a centred leap-frog scheme until a quasi-steady lee wave field is obtained. A further extension is the inclusion of a first-order (mixing-length) stability dependent turbulence closure scheme, which enables representation of the wind field within the boundary layer, and thus a prediction of the impact of lee waves on the near-surface flow. These extensions are described by King *et al.* (2004).

The 3DVOM code is used to generate detailed predictions of lee wave fields and associated near-surface winds. The simulations are typically based on background wind and potential temperature profiles, obtained from either radiosonde ascents or extracted from coarser resolution NWP model forecasts. In the past, the model predictions have been compared with observations of lee waves obtained during different research campaigns. Using an earlier version of the model Vosper and Worthington (2002) presented a detailed comparison of VHF radar measurements with the model predictions for a lee wave event over Wales and demonstrated close agreement. Vosper (2003) compared model vertical velocities with radiosonde ascent rate fluctuations over the Isle of Arran, southwest Scotland, over a 2 month period. The study demonstrated that in general the model wave amplitude predictions were well correlated with the observations. It was also shown how the model could provide an accurate description of the details of the wave field, with the phase of the wave motion being well represented. A form of the model has also been used to predict stratospheric wave motion over Scandinavia (Eckermann *et al.*, 2006). A further validation example, in which predictions of the current (terrain-following, plus turbulence scheme) version of the model have been compared with aircraft measurements, is provided below.

During October 2003 to April 2005 measurements of lee waves were made across the Pennines, a north–south ridge which extends through northern England. The experiment, described in detail by Sheridan *et al.* (2007), included a number of intensive observation periods, one of which involved *in situ* measurements of lee wave motion by the FAAM BAe-146 research aircraft. On 17 November 2004, during an episode of strong stable westerly flow, a series of vertically stacked horizontal flight legs was flown across the Pennines. These legs were orientated approximately east–west and were aligned with the wind direction measured at 2 km MSL, thus roughly perpendicular to the orography. The flight legs were conducted between 1047 and 1217 UTC over a height range of 1080–1950 m MSL. The track of the lowest of these legs is shown in Figure 1. Also shown in Figure 1 are radiosonde profile measurements made from an upwind site to the west of the Pennines (Hazelrigg, 54.01 °N 2.78 °W, near Lancaster) at 1035 UTC. These reveal a strong stable westerly flow through the troposphere. Wind speeds at 500 m MSL were approximately 20 m s^{-1} and these increased to 30 m s^{-1} at 5 km MSL. This positive shear over the lower troposphere gives rise to a decreasing profile of the Scorer parameter, $l^2 = N^2/U^2$, with height. Values of l^2 in the lowest 2–3 km are approximately 0.5 km^{-2}, whereas values above 5 km are close to zero. Such conditions, whereby a low-level layer of positive Scorer parameter is overlain by smaller values, allow the wave energy to be ducted horizontally, resulting in the formation

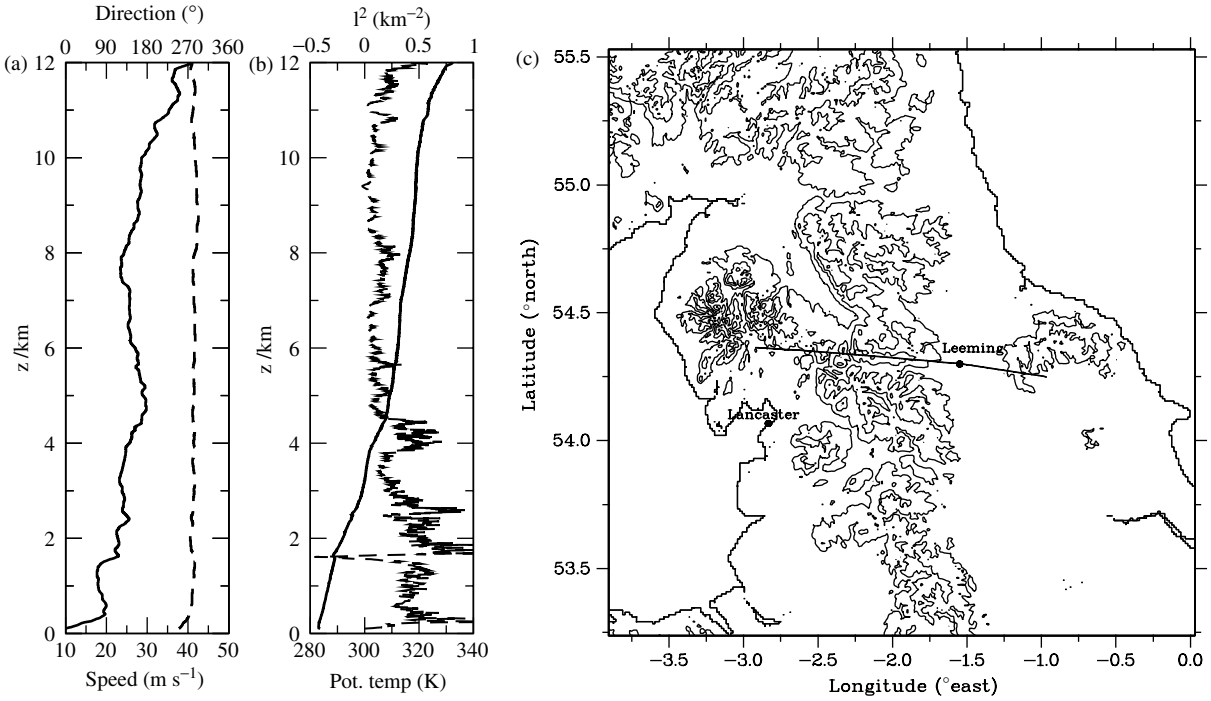

Figure 1. Radiosonde measurements of (a) wind speed (solid) and direction (dashed) along with (b) potential temperature (solid) and Scorer parameter, l^2 (dashed) for the 1035 UTC ascent from Hazelrigg, near Lancaster, on 17 November 2004. Panel (c) shows the flight track of the FAAM BAe146 aircraft along the lowest leg (1080 m MSL) across the Pennines during the same morning. Also shown are terrain height contours at 200 m intervals.

of trapped lee waves. The relative humidity in the 1035 UTC radiosonde was between 95 and 100% across a layer extending from 100 m to 2 km MSL. Similar moist layers were observed in later radiosonde releases at 1403 and 1614 UTC. Satellite imagery revealed extensive cloud cover across the UK during the day, with a marked wave signature in the cloud pattern, both over the Pennines and in other areas.

The non-dimensional mountain height, *NH/U*, for this case can be estimated from low-level radiosonde measurements. Assuming a mountain height of 750 m (approximately the greatest peak height encountered beneath the aircraft legs) and using the wind speed at 2 km and a bulk-average estimate of N computed from potential differences between 500 and 1000 m MSL, gives an estimate of $NH/U = 0.4$ for the 1035 UTC radiosonde. This value is significantly smaller than unity.

As shown in Figure 2, wave motion was observed above and to the lee of the Pennines along all aircraft legs. Peak vertical velocities exceeded 4 m s^{-1}. The fact that the peaks and troughs are aligned in the vertical suggests that the wave energy is trapped. Also shown are the model vertical velocity predictions for 1200 UTC. The latter were obtained from a 3DVOM simulation based on a 12 h forecast profile extracted from the Met Office global forecast model. The simulation was conducted with a 1 km horizontal resolution on a 256 × 256 km^2 domain which extended across the Pennines. The vertical grid consisted of 60 vertical levels, stretched so as to give higher resolution in the boundary layer. The lowest interior model level was at 10 m, and the grid spacing increased smoothly to approximately 450 m at the model upper boundary (located at 16 km).

Figure 2 shows that the model reproduces the observed wave motion to a reasonable degree of accuracy. Both the amplitude and horizontal wavelength of the vertical velocity fluctuations are captured and the phase of the waves, particularly over the western side of the hills, is well represented. Although clearly a more thorough investigation, involving a large number of cases, would be required in order to assess the general accuracy of the model properly, these results are nevertheless encouraging and, along with previous comparisons of the model with observations (e.g. Vosper and Worthington, 2002; Vosper, 2003), suggest that the model is well suited to provide forecast guidance over the UK, and could provide also useful climatological information. This is further confirmed in Section 4, where evidence for lee wave clouds in satellite imagery is correlated with predictions from the operational 3DVOM forecasts over a longer period.

3. The operational lee wave forecast system

The 3DVOM code forms the basis of a Met Office lee wave forecasting system, which has provided daily forecasts since 2006. Before November 2010, the system was run once *per* day, using Met Office global model forecast profiles from the 1800 UTC run at 6 h intervals to provide forecasts up to 48 h ahead. Since November 2010 the system has been upgraded so that forecasts are updated four times *per* day, using data from the global model 0000, 0600, 1200 and 1800 UTC forecast runs.

For the UK, the model is run for five separate mountainous or hilly areas. These are the Pennines and Lake District (northwest England), the Grampians (northern Scotland), the Mourne and Sperrin mountains (Northern Ireland), Snowdonia (north Wales) and Dartmoor (southwest England). The locations and extent of the model domains are shown in Figure 3. Additional model domains are also available for southern Ireland and the Falkland Islands in the south Atlantic, but results for these are not discussed in this paper.

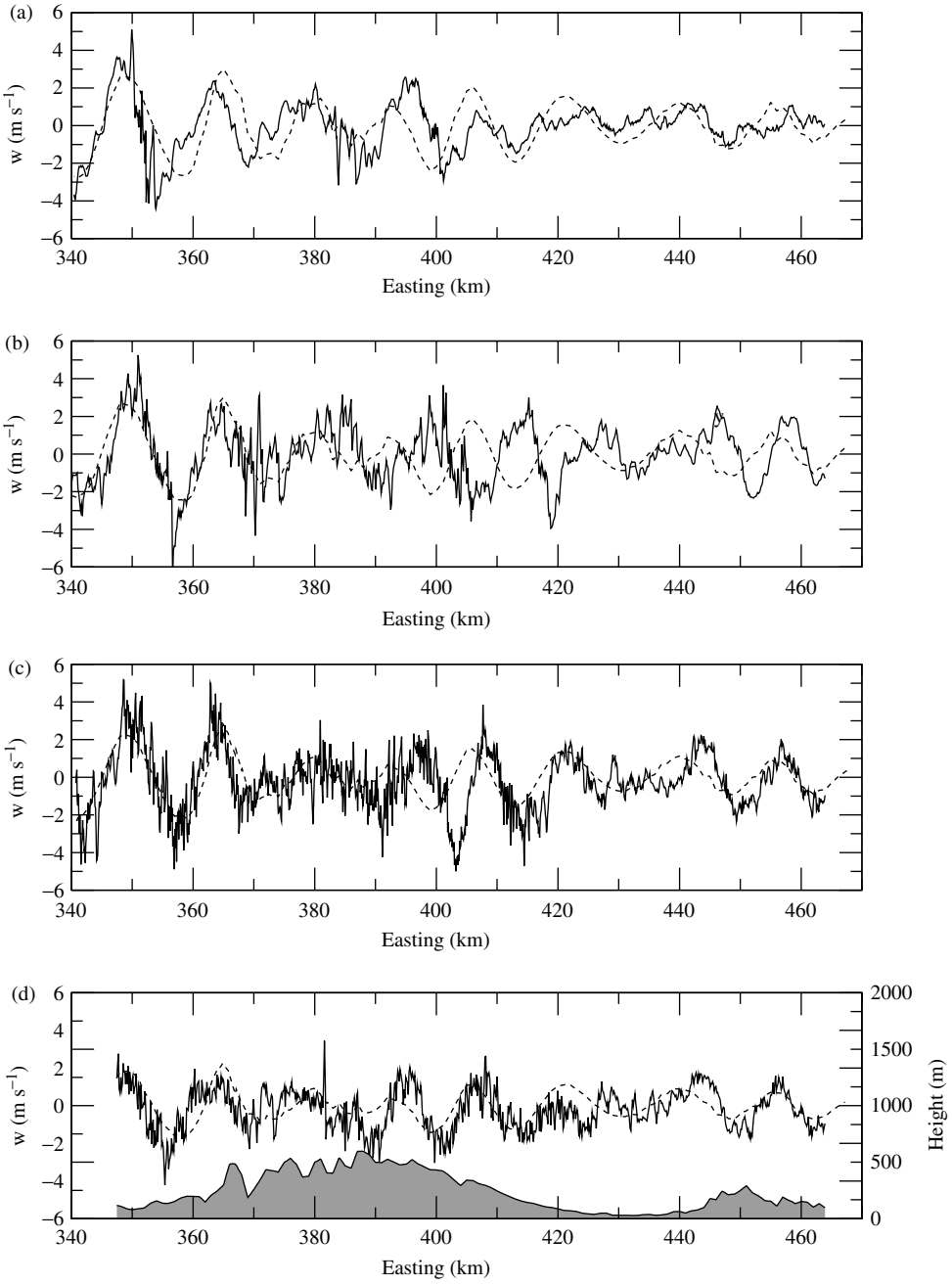

Figure 2. Vertical velocity measured by the FAAM BAe 146 aircraft (solid lines) along straight vertically stacked horizontal legs across the Pennines on 17 November 2004. The legs are at heights of (a) 1950 m, (b) 1650 m, (c) 1350 m and (d) 1080 m MSL. The start and end times of these legs are 1048–1110, 1202–1217, 1135–1158 and 1115–1130 UTC, respectively. Also shown are the 3DVOM vertical velocities (dashed lines), valid at 1200 UTC, along each leg. The model orography beneath the lowest leg is shown in (d).

For each of the above five UK domains the model is configured with a 1 km horizontal resolution. The upper boundary is placed at 16.5 km and a stretched vertical grid is used. The lowest grid level is at 2 m and the grid spacing increases smoothly with height, starting at 4 m at the ground and increasing to approximately 650 m at the upper boundary. Vertical profiles of wind, potential temperature and density are extracted from the global forecast model within each domain and interpolated onto this vertical grid. These profiles, the locations of which are shown in Figure 3, are then used to represent the background state. A separate 3DVOM run is conducted for each domain, using a different profile for every 6 h forecast time, from $T + 06$ h to $T + 48$ h. Each forecast is started from an initial state in which the wave perturbations are zero, and is run for an integration time of 3000 s, by which time the wave field is generally well established and is quasi steady. Note that the sub-division of the UK into separate independent domains means that interference effects, whereby waves generated in one region propagate sufficiently far that they interact with those generated in another, cannot be represented.

Whilst in principle it might be better to locate the forecast profiles upwind of the regions of interest, during initial testing of the forecast system, sensitivity tests suggested that the 3DVOM forecasts were insensitive to small changes in the profile locations. Given that the global model mid-latitude horizontal resolution was approximately 40 km at this time (and

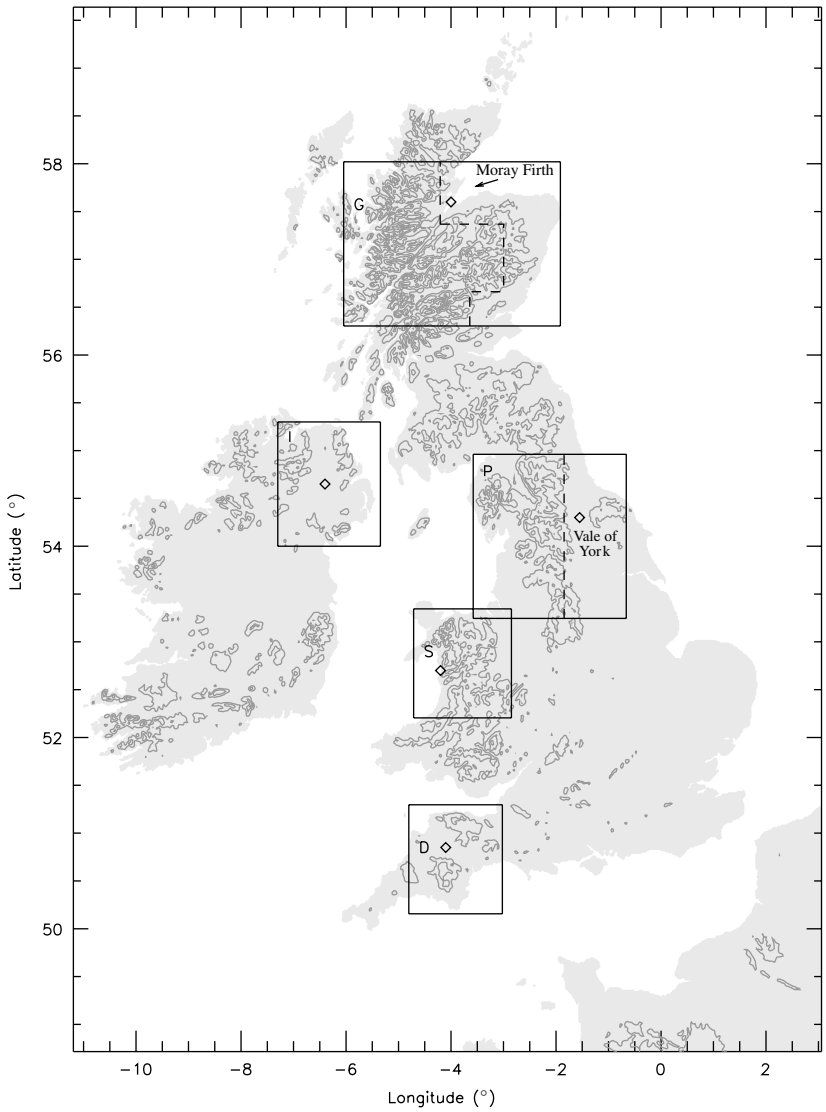

Figure 3. The location of the operational 3DVOM forecast domains over the UK. The labels 'G', 'I', 'P', 'S' and 'D' refer to the Grampians, Northern Ireland, Pennines, Snowdonia and Dartmoor domains, respectively. The diamonds mark the locations of the global model profiles used to represent the background flow for each domain. Also shown are terrain height contours (line contours) at an interval of 200 m. The dashed lines denote the boundaries of the sub-domains used in the surface wind analysis presented in Section 6. Also marked are the Vale of York and Moray Firth.

remained so for the analysis period considered in this study), this result is perhaps not surprising. The model's representation of orography at this coarse resolution is very poor and other than perhaps at low levels, the profiles are not greatly affected by their position relative to the mountains.

In this paper output from the forecasts over a 3 year period from 1 March 2007 to 28 February 2010 is analysed. The focus is only on results for the first 24 h of the daily 1800 UTC forecasts. The dataset therefore contains four forecasts *per* day (valid at 0000, 0600, 1200 and 1800 UTC). Due to the transition to a new data archive system there was a storage outage from 17 September 2009 to 28 November 2009, resulting in data loss from this period. With this exception, the archive is almost complete over the 3 year analysis period.

Of the five regions considered, the mountains are highest in the Grampians. Nonlinearity might therefore be expected to be relatively more important in this region, since *NH/U* values larger than unity are likely to occur with a greater frequency. In an attempt to quantify the extent to which the linear assumption will be a good approximation, distributions of *NH/U* were computed for each of the model domains. For each forecast profile a bulk value of N was calculated from potential temperature differences between heights of 500 m and 1 km MSL. The wind speed, U, was taken to be that at 2 km MSL. Rather than consider the maximum mountain height for each domain (which may be unrepresentative) the approach taken was to identify all local maxima in the model orography and assign a different value of H (and hence NH/U) to each individual mountain peak. A frequency distribution for *NH/U* can then be formed from the multiple values for each forecast over the 3 year analysis period.

The distribution of mountain heights, H, for the Grampians domain is shown in Figure 4(a). A broad range of heights is present in this region, with the majority of peaks in the model orography being less than 900 m high. The corresponding frequency distribution for *NH/U* is shown in Figure 4(b). Note that in order to restrict attention to the relevant lee wave situations, only data for which model vertical velocities

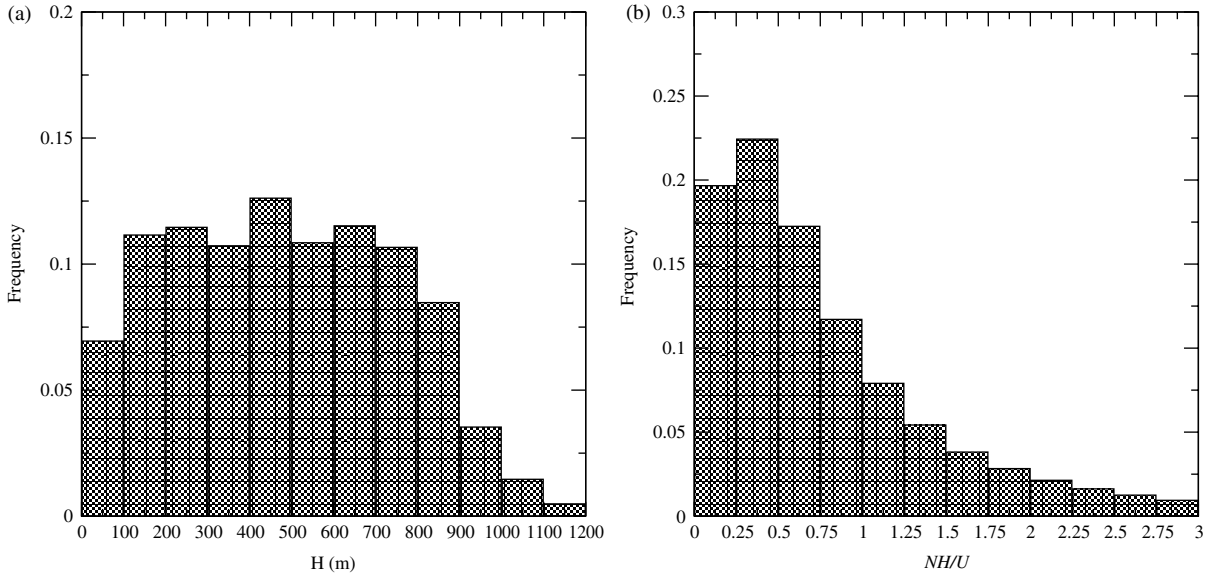

Figure 4. Frequency distributions for (a) the mountain heights, H, and (b) the non-dimensional mountain heights, NH/U, for the Grampians model domain. The NH/U distribution was calculated using all forecast profiles over the 3 year analysis period for cases where the maximum 3DVOM vertical velocity at 700 hPa exceeded 1 m s^{-1}.

at 700 hPa exceeded 1 m s^{-1} are included in this analysis. This is revisited in Section 4, where such measures of the vertical velocity are used to categorize the strength of lee wave cases. The most frequently occurring values of NH/U for the Grampians are less than unity, though the tail of the distribution clearly extends to larger values. Approximately 29% of the NH/U values are greater than unity, suggesting that nonlinear processes might be important for a significant number of cases. The distributions for the other four domains are similar, although the frequencies generally decay more rapidly with increasing NH/U. For Snowdon domain approximately 20% of NH/U values are greater than unity. The equivalent results for the Pennines, Dartmoor and Northern Ireland domains are 12, 4 and 7%, respectively. It seems likely, therefore, that the assertion made in Section 2 regarding NH/U for UK mountains, will be generally valid, although there will be a significant number of cases, particularly in the Grampians, Pennines and Snowdon regions where nonlinearity could play an important role.

4. Comparisons of operational lee wave forecasts with satellite imagery

Figure 5 shows the high-resolution (1 km) visible satellite image from the Meteosat Second Generation (MSG) satellite over the UK at 1200 UTC on 15 December 2009, alongside the forecast vertical velocity at 700 hPa (∼3 km MSL) for the Grampian region. At this time a high pressure region was situated just to the south of Iceland with a weak low pressure system over Scandinavia. This synoptic situation drives a north-easterly flow over Scotland. The Scorer parameter, $l^2(z)$, based on the $T + 18$ h global model forecast profile for the Grampians region, decreased sharply with height between 1.5 and 2.5 km

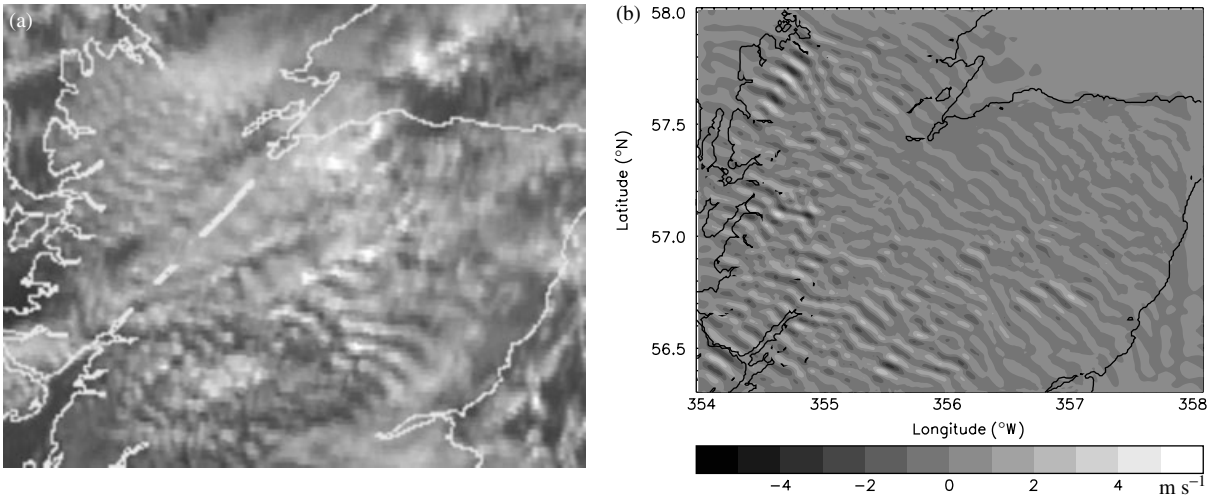

Figure 5. (a) A high resolution MSG visible satellite image from over the UK for 1200 UTC on 15 December 2009; and (b) the 18 h forecast of vertical velocity (m s^{-1}) at 700 hPa for the Grampians region, valid at the same time as the satellite image. The east–west and north–south dimensions of the model domain shown in (b) are 256 and 192 km, respectively.

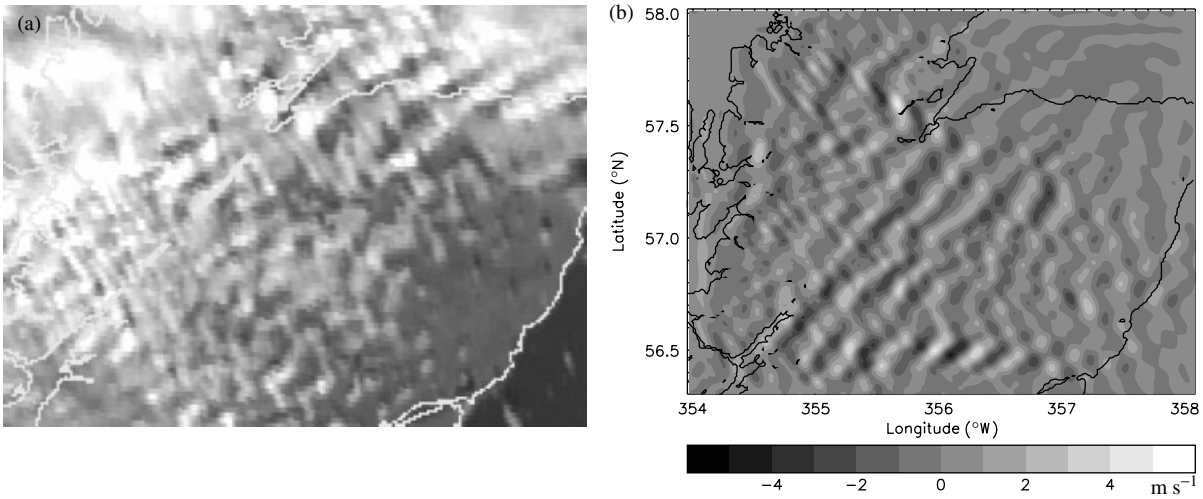

Figure 6. As for Figure 5, but for 1200 UTC on 19 November 2008.

from approximately 2.2–0.4 km^{-1}. This suggests that the conditions were conducive to wave trapping. The satellite image contains bands of lee wave clouds orientated perpendicular to the incident wind, with a horizontal wavelength of between 9 and 10 km. The orientation, horizontal wavelength and location of the waves forecast by the model are in good agreement with the waves seen in the satellite image. In this case the model forecasts high amplitude lee waves, with peak vertical velocities at 700 hPa in excess of 4 m s^{-1}.

Figure 6 shows the same fields as for Figure 5 but for a case on 19 November 2008 at 1200 UTC. In this case a low pressure region was situated to the northeast of Scotland, with high pressure over the mid-Atlantic. These conditions led to strong west-northwesterly flow across Scotland, with wind speeds of approximately 30 m s^{-1} at 2 km MSL. In this case l^2 decreased with height between 1 and 8 km, from approximately 0.5 km^{-1} to zero, again suggesting conditions suitable for wave trapping. The satellite image reveals lee waves with crests aligned southwest to northeast and horizontal wavelengths of around 18 km. Again the orientation, horizontal wavelength and location of the waves forecast by the model are in good agreement with the waves seen in the satellite image.

In order to confirm more generally that the instances of wave clouds in satellite imagery coincide with forecasts of lee wave events, satellite imagery has been examined for the whole 3 year period 1 March 2007 to 28 February 2010. High-resolution MSG images were visually inspected for the presence of lee wave clouds using all available daily visible imagery at 1200 UTC over the Grampians region. Images were available for much of this period although there were some significant periods of missing data (July 2007; 8 April 2008 to 28 August 2008 and September 2009). With the available imagery (891 days worth), clear cases of wave clouds were identified on 146 days i.e. on approximately 16.4% of days. For the remaining imagery, no clear-cut wave signature was identified, although this does not necessarily indicate wave clouds were absent. In many cases the images were either obscured by intervening (high) cloud or the cloud patterns lacked sufficient clarity to judge whether wave clouds were present.

Archived 3DVOM forecast data were available for 136 of the 146 days on which wave clouds were identified in the satellite imagery. For each forecast the quantity $|w|_{\max}$ was calculated, where $|w|_{\max}$ is defined as the maximum value of the magnitude of the vertical velocity anywhere in the domain at or above 700 hPa. This was used to assess whether lee waves were present in the forecasts. For 120 of the forecasts $|w|_{\max}$ exceeded 1 m s^{-1}, suggesting that significant wave motion was present. Of the remaining 16 days, smaller-amplitude lee waves were present in the model in 12 cases, with orientation of wave crests similar to those observed in the satellite images. There were only four cases where wave clouds were observed, but no waves were forecast. This analysis suggests that, for the Grampians at least, the model has a very high hit rate of approximately 97%. Note that the performance of the model did not appear to be dependent on incident wind direction. When the 136 days were categorized in terms of their cardinal wind direction (at 2 km MSL), there was no noticeable change in the hit rate.

Since an absence of wave clouds cannot be used to infer a lack of wave motion, it is not possible to use satellite imagery to estimate the model false-alarm rate. It is of course possible that the above high hit rates are merely a symptom of systematic over-prediction of wave activity. Note, however, that the overall frequency of 1200 UTC model forecasts for the Grampians in which $|w|_{\max}$ exceeded 1 m s^{-1} is approximately 57% over the 3 year period, which is significantly lower than the 97% hit rate.

5. A climatological analysis of the forecast lee waves

As in Section 4, the quantity $|w|_{\max}$ will be used to diagnose cases of wave activity in the model forecasts. Vertical velocities at lower heights are not used since close to the ground significant displacements can arise purely from mechanical lifting over the orography. Small-scale steep features in the terrain will generally force short-wavelength flow perturbations which decay exponentially with height and do not lead to wave motion. For example, in neutral stability flow perturbations will decay at a rate $\exp(-kz)$, where k is the horizontal wavenumber of the terrain feature. The magnitude of perturbations with a wavelength of 1 km will decay to negligible levels between the ground and 3 km (approximately 700 hPa). A wavelength of 4 km will decay by a factor larger than 10^{-2}.

An alternative method for automatically identifying lee waves in the forecasts would be to calculate the standard

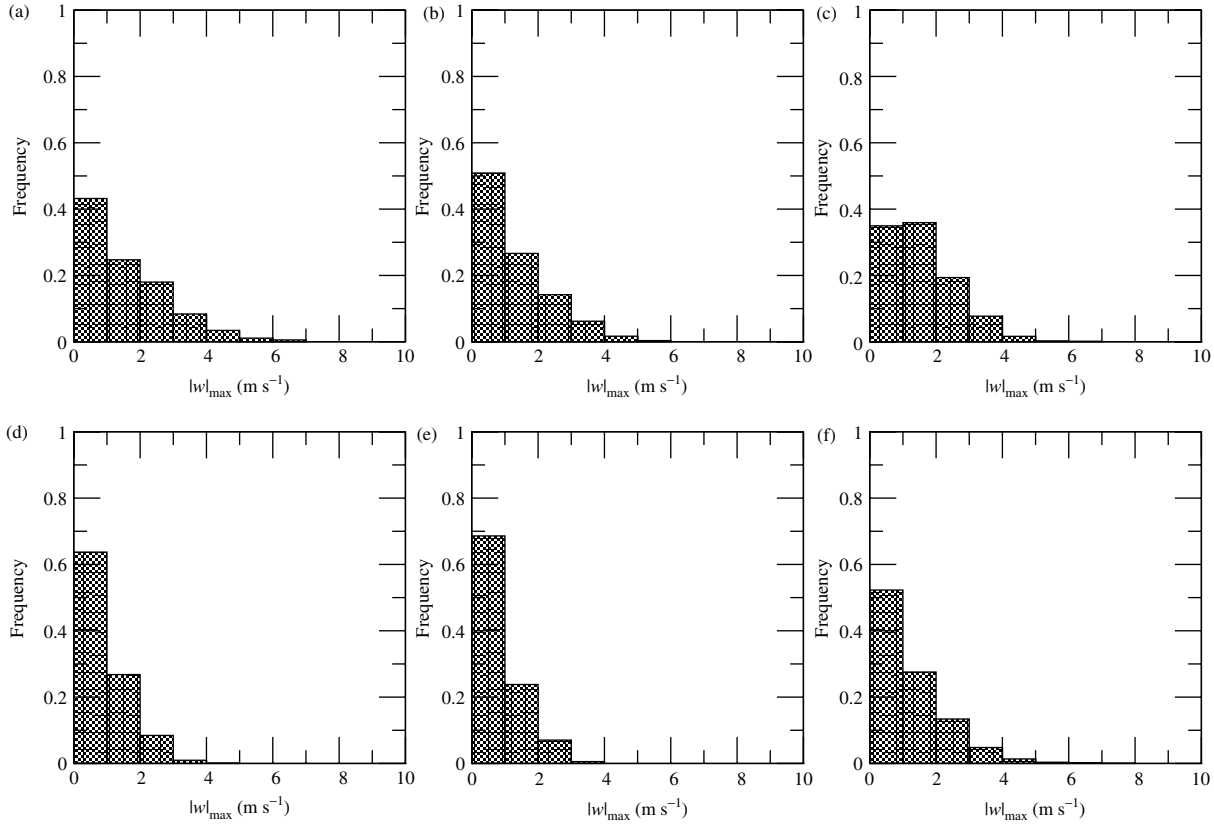

Figure 7. Frequency distributions for $|w|_{\max}$ in the (a) Grampians, (b) Pennines, (c) Snowdon, (d) Northern Ireland and (e) Dartmoor model domains over the 3 year period 1 March 2007 to 28 February 2010. The data have been binned into 1 m s^{-1} intervals. Panel (f) shows the distribution for all five domains.

deviation of the vertical velocity, σ_w, measured across the full model domain. Whereas $|w|_{\max}$ provides only a local measure of wave motion, σ_w also indicates how widespread the wave activity is and could in principle be used to differentiate between trapped and vertically propagating cases. Such an analysis would be complicated by the nature of the orography in each model domain, however, since the horizontal extent of the wave motion will depend to some extent on the proportion of the domain which contains orography. In this study, therefore, lee waves are diagnosed using $|w|_{\max}$ alone. Note, however, that at 700 hPa, σ_w and $|w|_{\max}$ are highly correlated. Over the 3 year period correlation co-efficients for the two measures are greater than 0.9 for all five regions.

Figure 7 shows frequency distributions for $|w|_{\max}$ for each of the five domains individually (Figure 7(a)–(e)) and for all domains together (Figure 7(f)). The data have been binned into 1 m s^{-1} intervals. There are noticeable variations in the frequency distributions. For the Northern Ireland and Dartmoor domains, the distributions exhibit a marked peak in the 0–1 m s^{-1} range and occurrences of $|w|_{\max}$ greater than 2 m s^{-1} are relatively rare. Over the Grampians, Pennines and Snowdonia domains the distributions have a longer tail and larger amplitude waves are relatively common. Interestingly, the distribution for Snowdonia is relatively flat at the lower end of the distribution ($|w|_{\max} < 2$ m s^{-1}). This is investigated further below.

In the following analysis, the wave amplitude for each forecast is categorized according to the size of $|w|_{\max}$. Forecasts in which $|w|_{max} \geq 1$ m s^{-1} are classified as lee wave cases. Additionally a further subset of forecasts is categorized as large-amplitude wave cases when $|w|_{\max} \geq 3$ m s^{-1}. This 3 m s^{-1} threshold corresponds to the Met Office aviation forecasting manual definition of severe wave activity.

Table 1 shows the frequency of occurrence of lee waves deduced using $|w|_{\max}$ for all five regions. The Snowdon and Grampian regions exhibit the most wave activity with lee waves forecast over 50% of the time, while the Dartmoor region exhibits the least wave activity (lee waves are forecast 31% of the time). Large-amplitude lee waves are forecast infrequently over both the Northern Ireland and Dartmoor domains, occurring in at most 1% of forecasts, but are relatively common in the Grampians where they are forecast 14% of the time. The frequency of lee wave events is correlated with the peak topographic height in each domain, with domains containing the highest peaks exhibiting wave activity on a more regular basis.

The seasonal variations of forecast lee wave activity are shown in Figure 8, where the frequencies are grouped by months. Figure 8(a) shows the seasonal variation of all lee wave cases for the five regions. Maximum activity occurs in the winter months, with lee waves being relatively less frequent in summer forecasts. For example, in winter (December to February) lee waves are forecast ($|w|_{\max} \geq 1$ m s^{-1}) across the Grampians 67% of the time, whilst in summer (July to August) this drops to 44%. Figure 8(b) shows the seasonal variation of the large-amplitude ($|w|_{\max} \geq 3$ m s^{-1}) lee wave cases. The inter-season variability is generally stronger for these. For example the Grampians region is forecast to have almost three times more large-amplitude lee wave cases in winter than in summer.

Table 1. The frequency of lee wave events and large-amplitude lee wave cases over the 3 year period 1 March 2007 to 28 February 2010, as deduced from $|w|_{\max}$ in the forecasts.

Model domain	Highest elevation (m)	Frequency of lee waves ($|w|_{\max} \geq 1$ m s^{-1})	Frequency of large-amplitude lee waves ($|w|_{\max} \geq 3$ m s^{-1})
Grampians (G)	1344	0.57	0.14
Snowdonia (S)	1085	0.65	0.10
Pennines (P)	978	0.49	0.08
Northern Ireland (I)	849	0.36	0.01
Dartmoor (D)	621	0.31	0.006

The highest elevation refers to the actual maximum terrain height (MSL) in each domain.

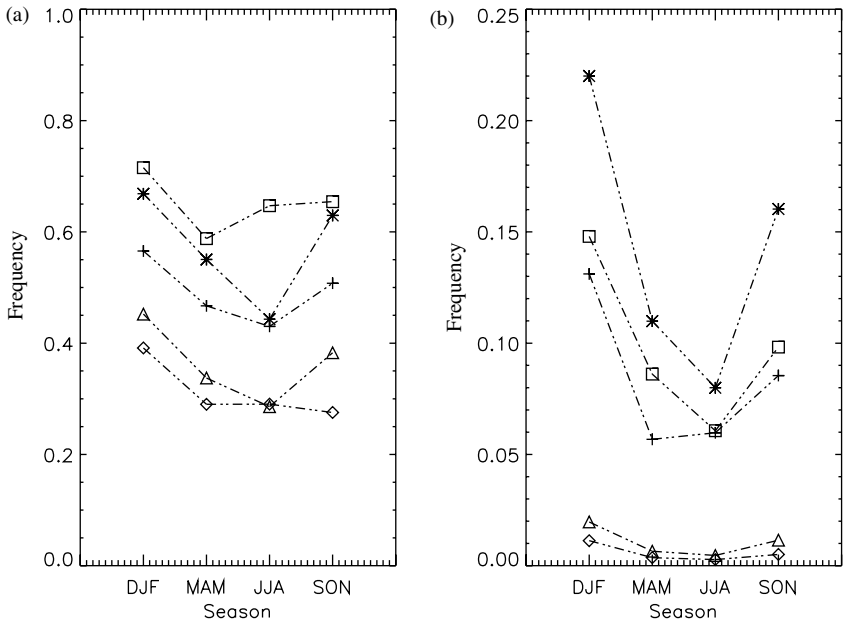

Figure 8. The seasonal frequency of (a) all lee wave cases (defined as $|w|_{\max} \geq 1$ m s^{-1}) and (b) large-amplitude lee waves ($|w|_{\max} \geq 3$ m s^{-1}) for the five model domains in the forecasts over the 3 year period 1 March 2007 to 28 February 2010. Results for the different domains are denoted by plus symbols (Pennines), asterisks (Grampians), diamonds (Dartmoor), triangles (Northern Ireland) and squares (Snowdon).

Table 1 and Figure 8(a) suggest that the behaviour across Snowdonia is somewhat anomalous compared to the other domains. The frequency of $|w|_{\max} \geq 1$ m s^{-1} events is relatively high, particularly during the summer months. To some degree this result is sensitive to the choice of the $|w|_{\max}$ thresholds. For example, choosing 1.5 m s^{-1} as the minimum vertical velocity reduces the frequency of lee wave cases over Snowdonia from 0.65 to 0.44, compared to 0.42 for the Grampians. Nevertheless, it does seem that small amplitude waves are relatively more common over Snowdonia than other areas and the high frequency of events during July to August is one contributing factor. This is perhaps related to the climatology of the wind in the region over the 3 year study period. Snowdonia experiences winds from southwesterly to westerly directions during July to August more often than the Grampians do. The forecast profiles at 2 km MSL exhibited these wind directions for 31% of Snowdon forecasts, compared with only 22% for the Grampians, whereas the frequencies for other seasons were more similar (within 2%). As demonstrated below, these wind directions are generally favourable for lee waves.

The extent to which a diurnal signal is present in the frequency with which lee waves appear in the forecasts has also been assessed. No notable or systematic variations were found. For example, for the summer months the frequency of lee wave events ($|w|_{\max} \geq 1$ m s^{-1}) varied typically by less than 10% across the four forecast times *per* day for all domains. This was also true for the large amplitude cases.

The forecast data have also been used to identify which conditions tend to be more conducive to wave formation. Figure 9(a) shows the relationship between $|w|_{\max}$ and the background wind speed, U, at 2 km MSL for the Pennines domain over the 3 year period. As expected, there is a clear relationship between the wave amplitude and wind speed, with larger amplitudes occurring in windy conditions. Figure 9(b) shows the relationship between lee wave activity and wind direction over the Pennines and indicates that the majority of larger wave events occur when the incident wind is from the west-southwest, with a secondary maximum in wave amplitude for northeasterly winds. Fewer large amplitude events occur for southeasterly or southerly flow. This dependence on wind direction is presumably principally due to the climatology of the incident flow, since stronger winds and stability occur more frequently during westerly flow regimes.

The extent to which the wave amplitude is affected by turning of the background wind in the lower troposphere has also been investigated. Figure 9(c) shows how $|w|_{\max}$ over the Pennines depends on the difference in wind direction, Δd, between heights of 4 and 1 km MSL. Clearly, the largest waves

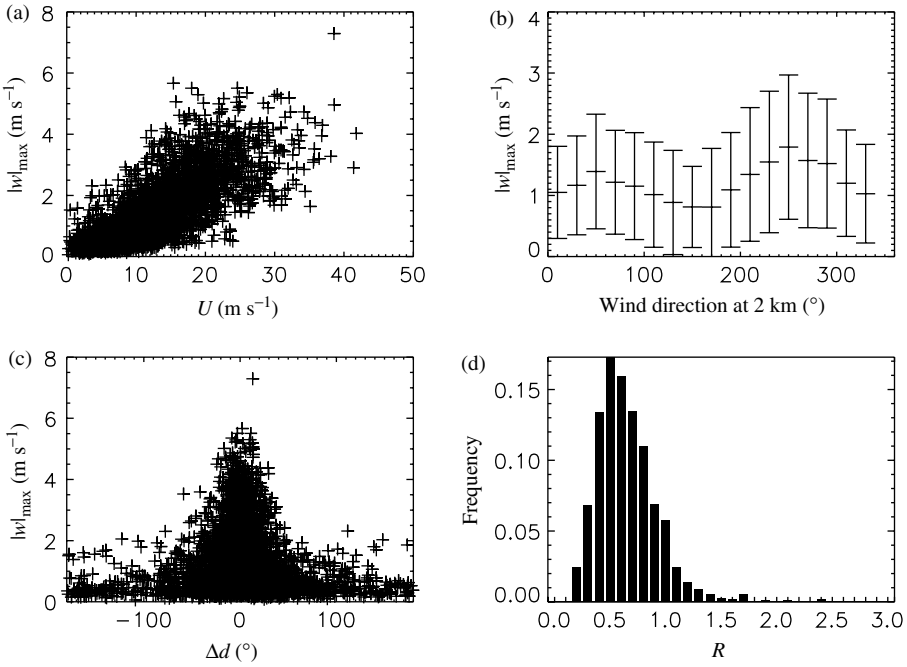

Figure 9. The variation of $|w|_{max}$ for the Pennines forecasts with (a) background wind speed, U, at 2 km, (b) wind direction at 2 km and (c) the difference in background wind direction, Δd, between heights of 4 and 1 km. Panel (d) shows the frequency distribution of the transmission parameter, R. Note that R is only calculated for cases where $|w|_{max} \geq 1$ m s^{-1}. Error bars in (b) indicate two standard deviations.

occur when there is little turning in the wind over this layer. Large changes in wind direction, particularly those greater than 90°, presumably lead to critical layer absorption (e.g. Shutts, 1995) for a large portion of the wave spectrum, resulting in reduced amounts of wave activity aloft.

The extent to which the forecast waves are trapped within the lower troposphere, as opposed to propagating vertically through the troposphere and into the lower stratosphere, has been investigated by defining a wave transmission parameter, R, as the ratio of the standard deviation of the vertical velocity, $\sigma_{w,}$ at 250 hPa (∼10 km) to that at 700 hPa (∼3 km). Values of R greater than unity are indicative of waves which grow with height, suggesting vertical propagation of energy. Smaller values imply wave trapping or critical layer absorption in the troposphere. The frequency distribution of R over the 3 year period for the Pennines region is shown in Figure 9(d). The peak close to 0.5 suggests that in the majority of cases the waves are partially trapped in the lower troposphere. However, the tail in the distribution for larger values of R also reveals a not insignificant proportion of cases where the waves are able to propagate throughout the troposphere. Note that basing the wave transmission parameter on the $|w|_{max}$ measure of vertical velocity, rather than the standard deviation, yields similar results to those shown in Figure 9(d).

The above relationships for $|w|_{max}$ have also been examined for the other domains. Figures 10 and 11 show the results for the Grampians and Snowdonia, respectively. The behaviours are similar to those seen over the Pennines. Notably the dependence of wave amplitude on wind speed and wind turning (Δd) resemble those observed for the Pennines, as do the frequency distributions for the trapping parameter R, suggesting that the wave propagation properties are common to all three domains. Similar results were also obtained for the Northern Ireland and Dartmoor forecasts (not shown). Note, however, that Figure 11(b) suggests again slight differences for Snowdonia: the variation of $|w|_{max}$ with wind direction is subtly different to those for the other domains. Other than for southerly flows, small vertical velocities over Snowdonia are relatively less common than for the Pennines and Grampians. For both westerly and easterly sectors the minimum end of the ranges of $|w|_{max}$ for Snowdonia are noticeably higher. This is consistent with the $|w|_{max}$ frequency distributions shown in Figure 7. Whilst it is not entirely clear why the wave generation over Snowdonia should be any more efficient than for other areas (for example the mean stability of the profiles does not appear significantly different to that of the other domains), it seems likely that this is related to some feature of the terrain shape. Perhaps the long south–north extent of the mountains along the Welsh coast, along with the significant mountains in northern Snowdonia, provides consistently large wave forcing for a larger span of wind directions than for the other domains. Combined with the higher frequency of westerly to southwesterly winds during the summer, this allows for more frequent wave generation.

6. The near-surface winds

In addition to the strong vertical winds which can be hazardous for aviation, wave motion can cause dangerous gusty conditions at ground level. Recent work (e.g. Doyle and Durran, 2002; Vosper *et al*., 2006) has shown, for example, how the pressure gradients associated with trapped lee waves can give rise to flow separation, leading to the formation of horizontally orientated vortices (lee wave rotors) beneath the wave crests. Small-scale vortices, embedded within these rotors, are thought to be responsible for severe turbulence and wind shear (Doyle and Durran, 2007). Downslope windstorms, in which the flow across the downwind foot of a mountain range undergoes significant acceleration, are also associated with large amplitude waves. In this case the waves are generally thought to be amplified through nonlinear processes, such as critical layer reflection (e.g. Klemp and Lilly, 1975; Peltier and Clark, 1979).

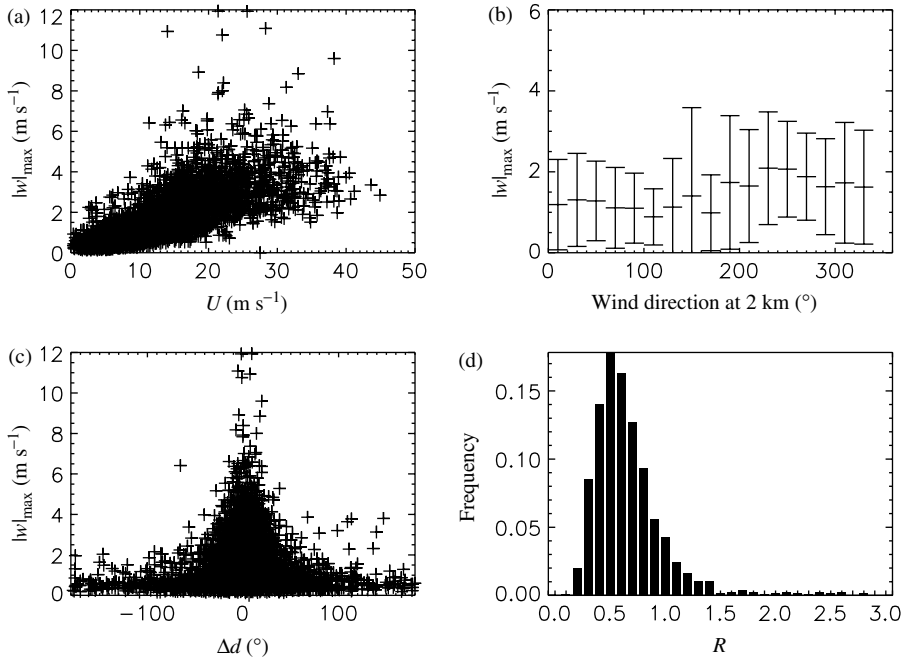

Figure 10. As for Figure 9 but for the Grampians model domain.

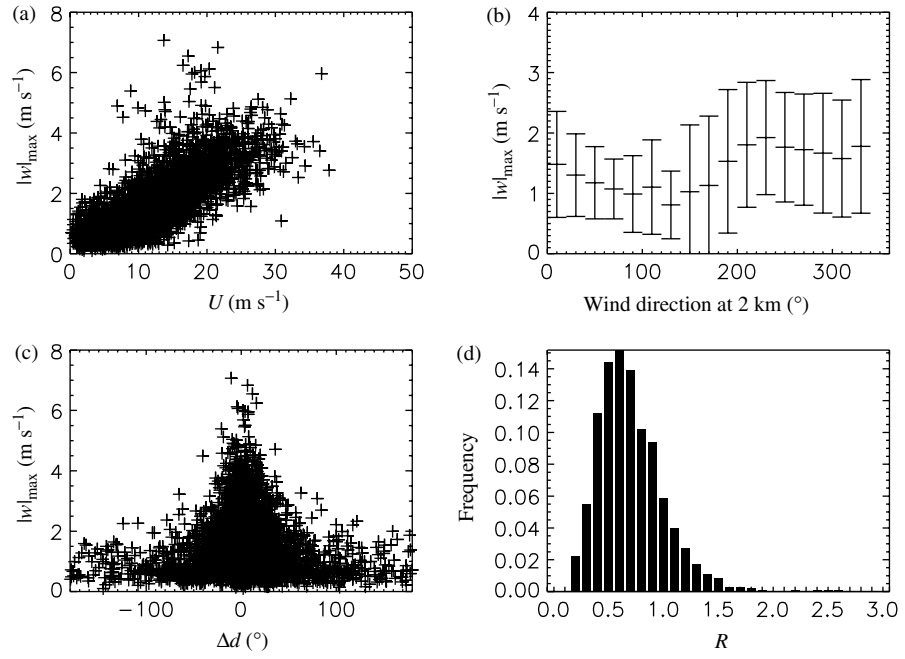

Figure 11. As for Figure 9 but for the Snowdonia model domain.

Since 3DVOM is a linear model with only a very simple representation of boundary layer processes, it cannot be expected to provide quantitatively accurate predictions of the near-surface flow. Clearly the model cannot represent the unsteady nature of turbulent gusts. Neither can it accurately predict the flow when the perturbations become large compared to the background flow quantities. However, the existence of large perturbations to the low-level flow may at least be a useful predictor of extreme conditions, even if the details of the model solution are inaccurate.

An example low-level flow field for which the model produced large accelerations is presented in Figure 12. This shows the 18 h forecast winds at 10 m during a period of strong westerly flow across the Pennines at 1200 UTC on 25 January 2008. In order to illustrate clearly the structure of the wind field, results are shown for a portion of the model domain only. The model predicted significant acceleration across the Pennines and also further to the east, across the cities of Leeds and Sheffield. Closer examination of Figure 12 reveals that to the north of the area the flow pattern to the east of the hills contains an alternate banded structure of enhanced and reduced wind speeds. This is an example of the low-level winds responding to the presence of a trapped lee wave aloft.

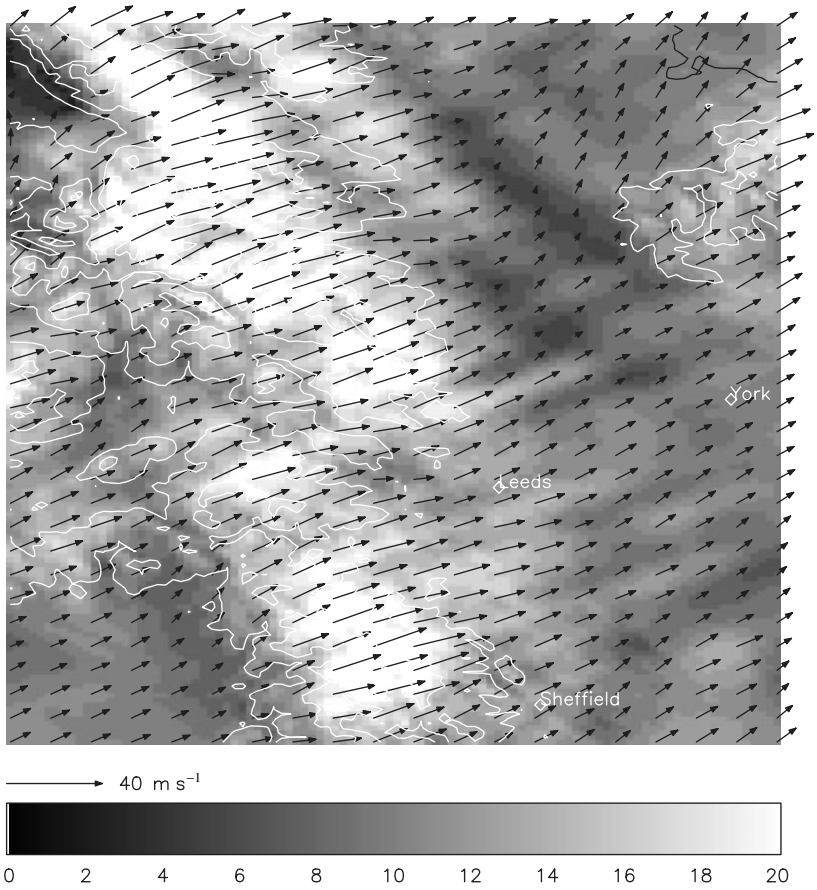

Figure 12. A close-up view of the forecast 10 m winds in an 18 h forecast for the Pennines region, valid at 1200 UTC on 25 January 2008. Solid lines mark the coastline. The shading denotes the wind speed (m s^{-1}). Terrain height contours are marked in white at 200 m intervals. The black contour marks the coastline. Also shown are the locations of the cities of Sheffield, Leeds and York to the east of the Pennines. The portion of the domain shown extends approximately 173 and 157 km in the east-west and north-south directions, respectively.

A further example of the behaviour of the model near-surface winds is presented in Figure 13. This shows the 18 h forecast vertical velocities at 700 hPa and 10 m winds for the Grampians at 1200 UTC on 19 November 2008: a case previously considered in Section 4. Again, for clarity, only a portion of the model domain is shown. Figure 13 shows how large changes in wind speed and direction occur beneath the troughs and crests of the trapped lee wave. Moving with the background flow (from the northwest to southeast, and approximately perpendicular to the southwest to northeast orientated phase lines), regions where the vertical velocity changes sign from negative to positive (Figure 13(a)) correspond to wave troughs. Wave crests coincide with regions where the vertical velocity changes sign from positive to negative. Figure 13(b) shows how the 10 m winds beneath the wave troughs are significantly accelerated, and are generally aligned with the background flow, with a westerly to northwesterly direction. On the other hand, beneath the wave crests the flow is considerably slower and is deflected. The wind direction beneath the crests is typically southerly or southeasterly. It is likely that in reality such rapid spatial changes in wind speed and direction would be associated with flow separation, and perhaps the formation of lee wave rotors. Recent evidence for this behaviour was obtained by Sheridan *et al*. (2007), who observed qualitatively similar flow patterns beneath lee waves downwind of the Pennines. Note that in a strictly two-dimensional flow, the occurrence of flow separation implies complete flow reversal (in a time-mean sense). The response of the low-level flow to the lee waves in three-dimensions is clearly much more complicated, as is the structure of the rotors (e.g. Doyle and Durran, 2007).

Although not shown here, results from a repeat of the above Grampians simulation in which lee wave effects were eliminated by replacing the height-varying potential temperature profile with a constant value (to give neutral stability) show very little variation in 10 m wind direction across the domain. Changes in wind speed are restricted to very localized areas across the mountain tops and valleys. The dramatic changes in the flow observed in Figure 13(b) are clearly related to the lee wave influence rather than a direct effect of the terrain complexity itself.

The more general characteristics of the near-surface flow variability in the forecasts are now examined. For each forecast the fractional speed-up parameter, $\Delta s(x, y)$, is calculated as $\Delta s = U_{10}(x, y)/U_{\mathrm{av}}$, where $U_{10}(x, y)$ and U_{av} are the spatially varying and area averaged 10 m wind speed, respectively. In order to concentrate on downwind effects, U_{av} and U_{10} are measured across sub-regions of the full model domains only, located to the east of the mountains and hence downstream of the orography in the prevailing westerly flow. The focus will be on the Pennines and Grampians forecasts. The sub-regions are shown in Figure 3 as the areas to the east of the dashed lines. They include the narrow inlet from Loch Ness to the sea (the Moray Firth) in the Grampians domain and the Vale of York to the east of the Pennines. Both areas are well-known for gusty conditions at ground level. Historically,

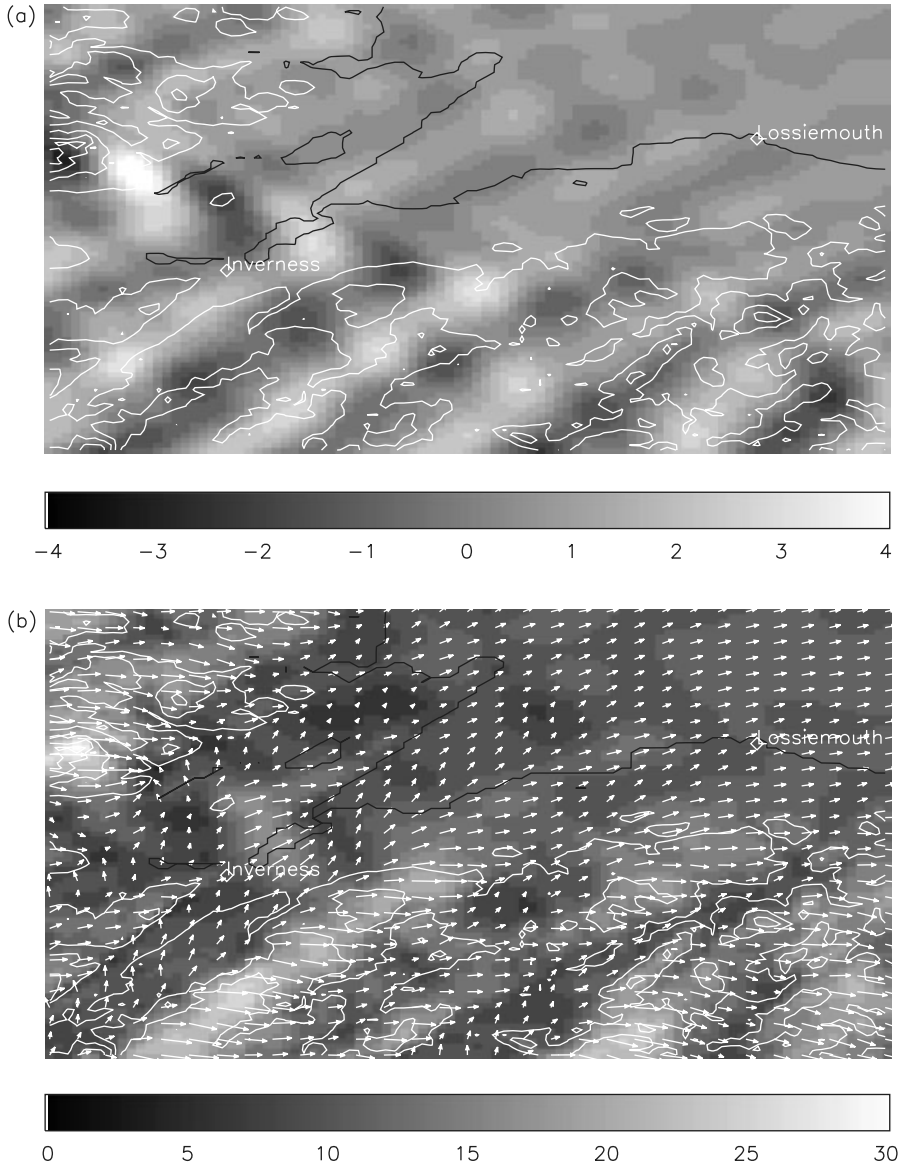

Figure 13. Close-up views of (a) vertical velocity (m s^{-1}) on the 700 hPa level and (b) 10 m winds in an 18 h forecast for the Grampians region, valid at 1200 UTC on 19 November 2008. The black contour marks the coastline. The shading in (b) denotes the wind speed (m s^{-1}). Also shown are the locations of the towns of Inverness and Lossiemouth. The portion of the domain shown extends approximately 93 and 90 km in the eastwest and north-south directions, respectively.

aircraft reports of severe turbulence in the Vale of York in conjunction with lee waves have been quite common (e.g. Cashmore, 1966).

Figure 14(a) shows a map of the locations of the maximum value of Δs attained in each forecast for the Pennines in which Δs exceeds 1.25 (a speed up of 25%) at at least one grid point. In order to avoid contamination from slack wind cases, results are only included when $U_{\mathrm{av}} > 5$ m s^{-1}. It appears that the locations of maximum acceleration are fairly widespread across the Vale of York area, although interestingly there is a cluster of points along a north–south orientated band, extending south of Leeming airfield (the site for the experiment presented by Sheridan *et al.*, 2007), roughly parallel to the Pennines and around 0.2–0.3° (∼13 to 20 km) from the eastern foot of the hills. This eastward displacement is presumably related to the typical horizontal wavelengths of the lee waves. It is noteworthy that this band of points lies close to a major trunk road, the A1 (marked in Figure 14(a)). Although relatively rare events, clusters of wind-related road accidents in which high sided vehicles are overturned have been identified on this section of the A1 (Walters and Finegan, 2009).

The equivalent map for the Grampians is shown in Figure 15(a). In this case the maximum fractional speedups are typically larger, so only data for forecasts where Δs exceeds 1.5 (a 50% speed up) are shown. In contrast to the Pennines, the large accelerations are generally concentrated within a small area. The points are clustered around the inlet between Loch Ness and the Moray Firth, near Inverness. The shape of the terrain presumably has a strong influence in this case and channelling of the flow through the inlet may further enhance the acceleration due to the lee waves.

In order to detect rotors, or at least the linear model representation of flow separation beneath wave crests, a suitable measurement is the degree of turning of the near-surface wind. The quantity $|\Delta\alpha(x, y)|$ is defined as the absolute difference

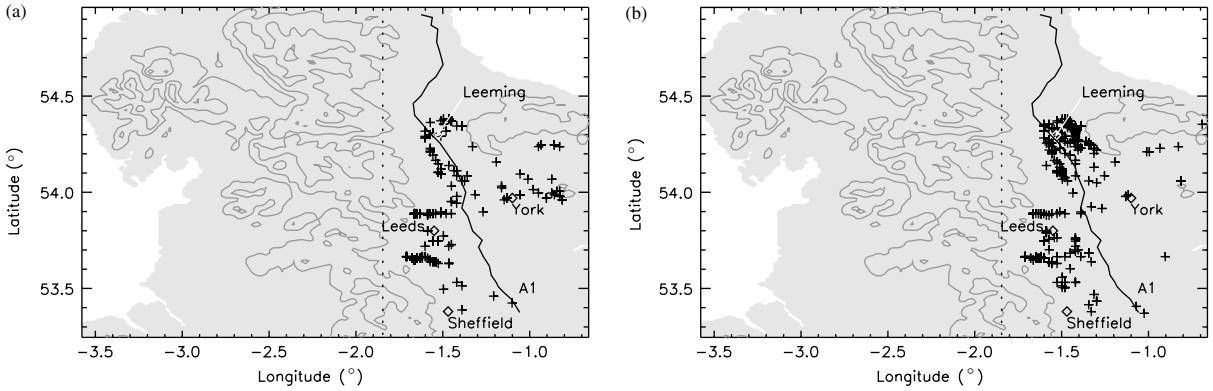

Figure 14. The location of (a) the maximum fractional speed-ups, Δs, in Pennines forecasts where the maximum values were greater than 1.25 and (b) the maximum values of the wind turning parameter $|\alpha|$, in forecasts where $|\alpha|$, exceeded 23°. In both cases the calculations were performed over the relatively flat sub-regions to the east of the dotted line. Results are shown only for forecasts in which the average 10 m wind speed across the sub-domain is greater than 5 m s^{-1}. Also marked are the locations of the major conurbations Sheffield, Leeds and York and the airfield at Leeming. The route of the A1 trunk road is also shown (solid line).

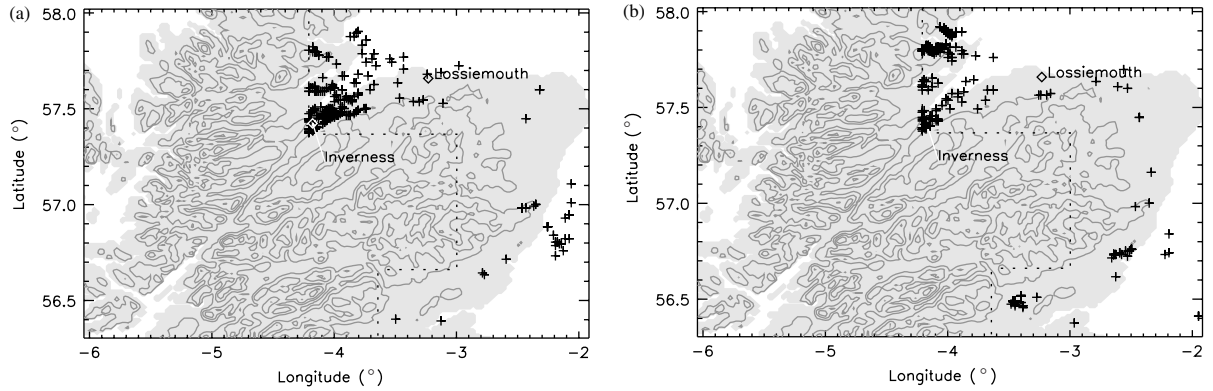

Figure 15. As for Figure 14 but for the Grampians region showing the location of (a) the maximum Δs values in forecasts for which $\Delta s > 1.5$ and (b) the maximum $|\alpha|$ points when $|\alpha|$ exceeded 94°. Also shown are the locations of the towns Inverness and Lossiemouth.

between the wind direction at every grid point and that of the area average wind vector. Again, only the downwind sub-regions of the domains are considered.

Figure 16 shows the relationship between the maximum value of the absolute vertical velocity on the 700 hPa surface, $|w|_{700}$ (as opposed to $|w|_{\max}$) and the maximum value of $|\Delta\alpha|$ in each forecast for the Pennines and Grampians. Again, only cases for which $U_{\text{av}} > 5$ m s^{-1} are included in the analysis. For both domains it appears that the maximum near-surface flow deflection increases with the maximum vertical velocity aloft. This is consistent with the idea that the amplitude of the lee waves (and associated pressure gradient) determines the size of the flow deflections at ground level. Note that the flow deflections are clearly much greater in the Grampians region. This is true for all vertical velocities and suggests that perhaps there are also other properties of the wave field, or local orography, which influence the low-level flow.

In order to identify individual cases of significant deflection, threshold values for $|\Delta\alpha|$ of 23° and 94° were chosen for the Pennines and Grampians domains, respectively. These correspond to the mean values plus two standard deviations in the 0–1 m s^{-1} $|w|_{700}$ bin. Figures 14(b) and 15(b) show the locations of the points of maximum $|\Delta\alpha|$ in forecasts for which $|\Delta\alpha|$ exceeds these critical values. Again, results are only shown when $U_{\text{av}} > 5$ m s^{-1}. In both domains there are clusters of points, indicating favourable locations for significant flow deflection by lee waves, and possibly rotor formation. These clusters are roughly co-located with those of the maximum accelerations (Figures 14(a) and 15(a)). Interestingly, the choice of the threshold value of $|\Delta\alpha|$ for the Pennines has resulted in multiple parallel bands of maximum flow deflection which run roughly parallel to the A1.

7. Summary

The 3 year archive of forecast data considered here allows a detailed picture of lee wave climatology to be established. Whilst the climatology is of course based on model data, rather than actual observations, the verification against satellite imagery and *in situ* measurements suggests that in general the model provides a realistic description of the lee wave fields. Furthermore, the high spatial and temporal resolution of the model datasets allows a far more detailed picture of the wave behaviour to be established than could be afforded through observations.

The analysis of model forecasts can be summarized as follows:

- Lee waves are relatively common over Scotland (Grampians), northern England (Lake District and Pennines) and north Wales (Snowdonia). Peak absolute vertical velocities are

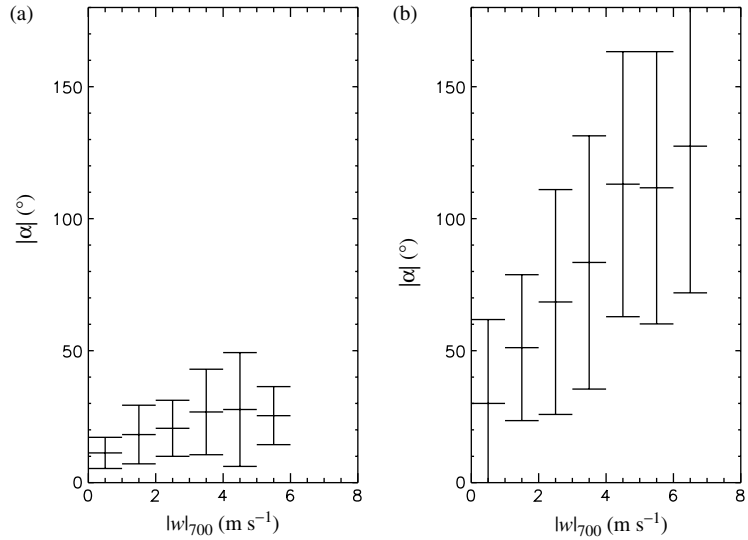

Figure 16. The maximum absolute difference in wind direction, $|\Delta\alpha|$, between the local 10 m and average flow across the downstream sub-regions of (a) the Pennines domain and (b) the Grampians domain (see Figure 3). The data are plotted against $|w|_{700,}$ the peak absolute vertical velocity on the 700 hPa surface. The central horizontal lines indicate the mean values of $|\Delta\alpha|$ for each $|w|_{700}$ bin and the error bars are two standard deviations long. Only data from cases in which $U_{av} > 5$ m s^{-1} were included in the analysis.

greater than or equal to 1 m s^{-1} at or above 700 hPa for these areas in 57, 49 and 65% of forecasts, respectively. Although larger-amplitude waves, where the peak absolute vertical velocities exceed 3 m s^{-1}, are less common, they are still observed in approximately 10% of forecasts for these areas.

- Vertical velocities of 1 m s^{-1} or more, at or above 700 hPa, occur in approximately 36 and 31% of forecasts for Northern Ireland and south-west England, respectively. However, large (greater than 3 m s^{-1}) amplitude lee wave cases for these regions are relatively rare and occur in only 1% or less of the forecasts.
- There is a marked seasonal dependence in forecast lee wave behaviour. Lee waves are less common in the summer (July to August) for all regions.
- There is a general trend for the lee wave amplitude to increase with increasing incident wind speed. The climatology of prevailing westerly winds across the UK therefore means that the larger amplitude waves tend to occur during westerly flow.
- The degree of turning of the incident wind profile has a marked effect on the wave amplitude. The largest waves occur when the wind turning in the lower troposphere is minimal.
- The ratio, R, of peak absolute vertical velocity in the upper troposphere (250 hPa) to that in the lower troposphere (700 hPa) is typically around 0.5, suggesting that the forecast waves over the UK are usually partially trapped within the troposphere. However, the tail of the frequency distribution of R is long, and extends beyond unity, suggesting that for a significant number of cases the wave energy will propagate into the stratosphere.

Of course, it is important to recognize that deficiencies in the model might adversely affect the realism of the model climatology and the quality of the wave forecasts. For example, moist and nonlinear effects, which are absent in the model, might have an important influence on the wave amplitude and wavelengths. The importance of these effects may vary regionally. Whilst the analysis of forecast waves against satellite imagery suggests the model has a high level of skill in predicting lee wave events, a much more detailed analysis would be required to determine whether the correct wavelength and phase line orientation is captured. Further work is clearly required to address these questions.

Analysis of the model near-surface winds must also be treated with some caution, because of the nonlinear and turbulent nature of the flow, which will not be well represented by the model. However, under the assumption that the model is a predictor of extreme events (even if the predictions may not be quantitatively reliable), then some interesting and potentially valuable properties of the flow can be deduced from the model forecasts. For the Grampians and Pennines forecasts, there appear to be preferred areas where the low-level winds undergo significant acceleration due to lee waves. Analysis of the flow deflection beneath the wave crests suggests that this is also true for flow separation (and hence lee wave rotor formation). To the east of the Pennines the flow acceleration and rotor locations are generally situated within the Vale of York, and tend to lie along bands orientated roughly parallel to the hills to the west. The A1 trunk road and Leeming air base appear to lie within the favoured hotspot region. For the Grampians forecasts, significant acceleration and flow deflections are concentrated near Inverness and the inlet to the Moray Firth.

Verification of the above findings for the surface winds is beyond the scope of this work, but is clearly desirable. Whilst the synoptic network of automatic weather stations might be of some help in this regard, it seems likely that high spatial resolution would be required in order to establish a detailed picture of the influence of lee waves at ground level.

References

Cashmore RA. 1966. Severe turbulence at low levels over the United Kingdom. *Meteorol. Mag.* **95**: 17–18.

Doyle JD, Durran DR. 2002. The dynamics of mountain-wave induced rotors. *J. Atmos. Sci.* **59**: 186–201.

Doyle JD, Durran DR. 2007. Rotor and sub-rotor dynamics in the lee of three-dimensional terrain. *J. Atmos. Sci.* **64**: 4202–4221.

Durran DR. 1992. Two-layer solutions to Long's equation for vertically propagating mountain waves: how good is linear theory? *Q. J. R. Meteorol. Soc.* **118**: 415–433.
Durran DR, Klemp JB. 1982. The effects of moisture on trapped mountain lee waves. *J. Atmos. Sci.* **39**: 2490–2506.
Eckermann SD, Doernbrack A, Vosper SB, Flentje H, Mahoney MJ, Bui TP, Carslaw KS. 2006. Mountain wave-induced polar stratospheric cloud forecasts for aircraft science flights during SOLVE/THESEO 2000. *Weather Forecast.* **21**: 42–68.
Galvin JFP. 2009. Wave clouds. *Weather* **60**(4): 112.
Galvin JFP, Owens R. 2006. Mountain waves over the UK. *Weather* **61**(9): 254.
Galvin JFP, Page A, Tullett M. 2006. Lee waves over Ireland. *Weather* **61**(12): 362.
Grubišić V, Billings BJ. 2008. Climatology of the Sierra Nevada mountain-wave events. *Mon. Weather Rev.* **136**: 757–768.
Grubišić V, Doyle JD, Kuettner J, Mobbs S, Smith RB, Whiteman CD, Dirks R, Czyzyk S, Chon SA, Vosper S, Weissmann M, Haimov S, De Wekker SFJ, Pan LL, Chow FK. 2008. The Terrain-induced Rotor Experiment: an overview of the field campaign and some highlights of special observations. *Bull. Am. Meteorol. Soc.* **89**: 1513–1533.
King JC, Anderson PS, Vaughan DG, Mann GW, Mobbs SD, Vosper SB. 2004. Wind-borne redistribution of snow across an Antarctic ice rise. *J. Geophys. Res.* **109**: D11104.
Klemp JB, Lilly DK. 1975. The dynamics of wave-induced downslope winds. *J. Atmos. Sci.* **32**: 320–339.
Lester PF. 1978. A lee wave cloud climatology for Pincher Creek, Alberta. *Atmos. Ocean* **16**(2): 157–168.
Mobbs SD, Vosper SB, Sheridan PF, Cardoso R, Burton RR, Arnold SJ, Hill MK, Horlacher V, Gadian AM. 2005. Observations of downslope winds and rotors in the Falkland Islands. *Q. J. R. Meteorol.* **131**: 329–351.
Nance LB, Durran DR. 1998. A modelling study of nonstationary mountain lee waves. Part II: nonlinearity. *J. Atmos. Sci.* **55**: 1429–1445.
NTSB. 1992. United Airlines Flight 585, Boeing 737-291, N99UA, uncontrolled collision with terrain for undetermined reasons, 4 miles south of Colorado Springs, Colorado, March 3, 1991. AAR-92-06, PB92-910407. National Transportation Safety Board: Washington, DC; 160 pp.
NTSB. 1993. In-Flight Engine Separation Japan Airlines, Inc., Flight 46E Boeing 747-121, N473EV, Anchorage, Alaska, March 31, 1993. AAR-93-06, PB93-910407. National Transportation Safety Board: Washington, DC; 103 pp.
Peltier WR, Clark TL. 1979. The evolution and stability of finite-amplitude mountain waves. Part II: surface wave drag and severe downslope windstorms. *J. Atmos. Sci.* **36**: 1498–1529.
Sheridan PF, Horlacher V, Rooney GG, Hignett P, Mobbs SD, Vosper SB. 2007. Influence of lee waves on the near-surface flow downwind of the Pennines. *Q. J. R. Meteorol. Soc.* **133**: 1353–1369.
Shutts GJ. 1995. Gravity wave drag parameterization over complex terrain: the effect of critical level absorption in directional wind shear. *Q. J. R. Meteorol. Soc.* **121**: 1005–1021.
Shutts GJ, Healey P, Mobbs SD. 1994. A multiple sounding technique for the study of gravity-waves. *Q. J. R. Meteorol. Soc.* **120**: 59–77.
Shutts GJ, Vosper SB. 2011. Stratospheric gravity waves revealed in NWP model forecasts. *Q. J. R. Meteorol. Soc.* **137**: 303–317.
Smith RB. 1980. Linear theory of stratified hydrostatic flow past an isolated mountain. *Tellus* **32**: 349–364.
Smith RB. 1988. Linear theory of stratified flow past an isolated mountain in isosteric co-ordinates. *J. Atmos. Sci.* **45**: 3889–3896.
Vosper SB. 2003. Development and testing of a high resolution mountain-wave forecasting system. *Meteorol. Appl.* **10**: 75–86.
Vosper SB. 2004. Inversion effects on mountain lee waves. *Q. J. R. Meteorol. Soc.* **130**: 1723–1748.
Vosper SB, Mobbs SD. 1996. Lee waves over the English Lake District. *Q. J. R. Meteorol. Soc.* **122**: 1283–1305.
Vosper SB, Sheridan PF, Brown AR. 2006. Flow separation and rotor formation beneath two-dimensional trapped lee waves. *Q. J. R. Meteorol. Soc.* **132**: 2415–2438.
Vosper SB, Worthington RM. 2002. VHF radar measurements and model simulations of mountain waves over Wales. *Q. J. R. Meteorol. Soc.* **128**: 185–204.
Walters O, Finegan P. 2009. Identification of network locations and areas affected by high winds. Development of a network sensitivity model. Final Report, Issue D, July 2009. http://www.highways.gov.uk (accessed 25 October 2011).